
Beyond Timesteps: A Novel Activation-wise Membrane Potential Propagation Mechanism for Spiking Neural Networks in 3D cloud

Jian Song¹ Boxuan Zheng¹ Xiangfei Yang¹ Donglin Wang¹

Abstract

Due to the similar characteristics between event-based visual data and point clouds, recent studies have emerged that treat event data as event clouds to learn based on point cloud analysis. Additionally, some works approach point clouds from the perspective of event vision, employing Spiking Neural Network (SNN) due to their asynchronous nature. However, these contributions are often domain-specific, making it difficult to extend their applicability to other intersecting fields. Moreover, while SNN-based visual tasks have seen significant growth, the conventional timestep-wise iterative activation strategy largely limits their real-world applications by large timesteps, resulting in significant delays and increased computational costs. Although some innovative methods achieve good performance with short timesteps (< 10), few have fundamentally restructured the update strategy of spiking neurons to completely overcome the limitations of timesteps. In response to these concerns, we propose a novel and general activation strategy for spiking neurons called **Activation-wise Membrane Potential Propagation (AMP2)**. This approach extends the concept of timesteps from a manually crafted parameter within the activation function to any existing network structure. In experiments on common point cloud tasks (classification, object, and scene segmentation) and event cloud tasks (action recognition), we found that AMP2 stabilizes SNN training, maintains competitive performance, and reduces latency compared to the traditional timestep-wise activation paradigm.

1. Introduction

Recently, point cloud analysis gains significant attention across multiple fields due to its broad applications in autonomous driving (Cui et al., 2022), virtual and augmented reality (Mei et al., 2024; Zielinski et al., 2024), and robotics perception (Duan et al., 2021; Cheng et al., 2022). A point cloud, represented as a collection of points $P \in \mathbb{R}^{N \times D}$, typically describes the geometrical structure of certain objects and scenes. Clouds exhibit themselves in a sparse, uneven, and unordered distribution. Building upon these characteristics, point-based learning and voxel-based convolution (Wu et al., 2015) are two main paradigms. Point-based methods propose to learn features directly from raw input point clouds, e.g., PointNet (Qi et al., 2017a) proposed a unified MLP architecture for tasks ranging from classification to segmentation. PointNet++ (Qi et al., 2017b) expanded this idea further in a hierarchical network to deal with both local and global representations respectively. On the other hand, (Ma et al., 2022) pointed out that many efforts have been laid on local feature extractors with the deeper analysis of point cloud, heavily relying on sophisticated strategies to exploit geometric properties. This emphasis on complicated networks, although bringing improvement in performance, also results in prohibitive computations that restrict applications in natural scenes.

In addition to point cloud data, event-driven data, especially those captured by dynamic vision sensors (DVS), have been regarded as emerging asynchronous pseudo point clouds due to similar characteristics. While DVS resembles the conventional CMOS-sensor camera, it operates on an event-oriented mechanism, i.e., only a pixel detecting certain polarity changes in brightness will trigger a stream of events corresponding to that pixel asynchronously, rather than capturing the whole frame at once. Depending on whether the activation function utilizes a spiking mechanism, methods addressing recognition can be categorized into Artificial Neural Networks (ANN) and Spiking neural networks (SNN). (Lee et al., 2014) simultaneously used leaky integrate-and-fire neurons (LIF) as feature extractor and hidden Markov models as classification heads. LIF can zero out certain features like dropout, but this behavior is learned from an iterative decaying of input and past in-

¹School of Engineering, Westlake University, Hangzhou, China. Correspondence to: Donglin Wang <wang-donglin@westlake.edu.cn>.

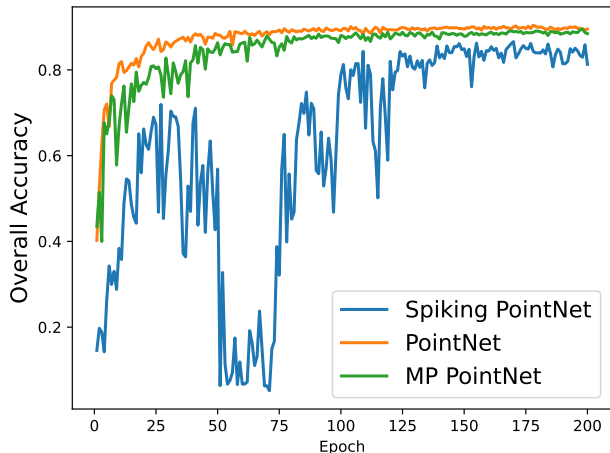


Figure 1. Classification accuracy on the ModelNet40 validation set without voting for each epoch during training. The models compared are MP PointNet (using AMP2), Spiking PointNet (Ren et al., 2023a) (SNN baseline, $T = 1$), and PointNet (ANN baseline). Each model was trained for 200 epochs.

formation, instead of being random. However, there is an often overlooked fact that most SNN methods neglect the spatial sparsity and temporal asynchrony of event streams, they count on the repeated activation through synchronous simulation. This raises an unfathomable parameter T , the optimal number of activation repetition, also known as time steps, to achieve the best performance.

Based on spiking activation, some studies have developed high performance network. Spike-Driven Transformer (Yao et al., 2023a; 2024a;b) continually optimized the architecture design of network. Spikformer series (Zhou et al., 2023; 2024) proposed spiking self attention and introduced a convolution-attention mixed mechanism to achieve event-driven computation. MS-ResNet (Hu et al., 2024), RG-CNN (Bi et al., 2020), RM-SNN (Yao et al., 2023b) implemented evaluation across various benchmarks including DVS128 Gesture, UCF101-DVS and HMDB51-DVS. As P3D ResNet (Qiu et al., 2017) implements pseudo-3D convolution for video, it is natural to consider event streams as a 3D spatial-temporal representation of scenes to learn. Spiking mechanisms ensure that the network discriminates between feature importance, retaining the most relevant features and discarding those of lesser significance. However, SNNs receive mixed reviews from academia due to gradient instability, mediocre performance, and a lack of hardware validation for low power consumption in most studies. Moreover, the iterative activation procedure derived from SNNs tend to leverage large time steps, which normally leads to a marginal improvement of 1-4%. Nevertheless, concurrently, the computation time extends markedly with the depth of

the network. Given that lessons from point cloud analysis can inspire DVS data processing, employing SNNs to facilitate effective and efficient computations of pseudo-event data is a logical progression.

How to maintain competitive performance and succinct design in networks seems a promising direction to explore. In this paper, we aim to build a simple and effective network training strategy for 3D vision tasks, inspired by spiking mechanism and residual feed-forward MLP, without relying on dedicated feature extractors increasing computation time steps. We term this strategy as **Activation-wise Membrane Potential Propagation (AMP2)**, The Spiking PointNet using AMP2 is referred to as **Membrane Potential PointNet (MP PointNet)**. By doing so, we alleviate the issue of training instability caused by the inherent discreteness of SNN shown in Figure 1. Meanwhile, this strategy could fully enjoy the advantages of existing highly-optimized MLP networks. Even in specific scenarios, AMP2 could eliminate the need to add a time dimension to the data and avoiding iterative nonlinear activation.

2. Related Work

In this section, we review representative works that analyze 3D data by cross-domain inspiration, applied in recognition tasks including action detection, hand gesture recognition, human pose estimation, as well as the analysis of 3D shapes of synthesized and real-world objects and scenes. Given a group of event stream containing I events, Event streams E , in other words, event points $\{e_i\}_{i=1}^I$ is represented as:

$$E = \{e_i\}_{i=1}^I = \{t_i, x_i, y_i, p_i\}_{i=1}^I \quad (1)$$

Where (x_i, y_i) denotes the position of pixel where the i th event occurs, t_i records the timestamp of the i th event, and p_i indicates changes of light intensity.

As frame-captured RGB image and event-recorded DVS data are closely related, the utilization of event-driven data in practical analysis also has been technically categorized into two approaches: using the event point and compressing events into frames. Point-based network takes carefully selected events (x, y, t) as input points, whereas frame-based method needs to densify I events into N images by integrating points through t . Frame representations of event clouds can be easily transferred back into non-event feature extractors mentioned in Section 1. Because event clouds $\{e_i\}_{i=1}^I$ will be replaced by the virtual image sets in shape of $\{T_i, C_i, H_i, W_i\}_{i=1}^N$, at the expense of response time, massive data volumes and increased computational costs. Regardless of drawbacks, this strategy still receives wide application in community for its convenience. EventMix (Shen et al., 2023) designed an efficient 3D mask strategy to achieve data augmentation on event frames.

2.1. Event Point-based Recognition

To fully explore the space-time sparsity and structure of the event points, (Wang et al., 2019) treated event set E as space-time event cloud P , regarding the timestamp t_i as a numerical measurement instead of sequential information. They trained a PointNet++ classifier using a rolling buffer mechanism in an end-to-end way. This strategy outperformed the CNN approach (Amir et al., 2017) achieving an accuracy of 97.08% compared to 96.49% on the 10-category recognition task of DVS128 Gesture. Meanwhile, EventNet (Sekikawa et al., 2019), a recursive version of PointNet, employed a temporal encoding layer prior to the symmetry function. EventNet demonstrated impressive results in ego-motion estimation and scene segmentation of event cameras. Still following PointNet design, the sequential relationship of event points was considered in ST-EVNet (Wang et al., 2020). Therefore, ST-EVNet abandoned MLPs and instead adopted space-time convolution kernels to learn local temporal features, resulting in a lower accuracy of 90.52% on DVS128 Gesture but with lower FLOPs per prediction. Subsequently, TTPoint (Ren et al., 2023b) argued that previous point-based studies suffer from inefficient sampling. It further improved on PointNet++ by stacking residual blocks within its extractors, achieving a performance of 98.8%. A spiking version of TTPoint, named SpikePoint (Ren et al., 2023c) was developed shortly after, reporting a competitive accuracy of 98.74% with 16 timesteps on the same benchmark.

2.2. 3D Recognition with SNN

Compared to 2D images, the sparse nature of point cloud poses more challenging obstacles when applying SNN. That is to say, larger timesteps are required to accumulate enough spikes during the forward propagation of training. The breakthrough in spike-driven analysis of point clouds was made by (Lan et al., 2023) and (Ren et al., 2023a), which almost simultaneously obtained spiking versions of PointNet through ANN-SNN conversion and direct training based on surrogate gradients, respectively. Inspired by adaptively adjusting spiking parameters for image classification, the former implemented an adaptive threshold and activation mechanism in ANN-SNN conversion for PointNet, while the latter developed a trained-less but learning-more method for timestep decision to mitigate the increasing time cost of training. Furthermore, this work suggests that the iterative computation with long timesteps essentially enhances the model’s generalization ability. (Wu et al., 2024) introduced a residual network, P2SResLNet, that combined integrate-fire (IF) neurons and 3D kernel point convolution of Convoke (Thomas et al., 2019). However, P2SResLNet failed to match the performance of its baseline KPConv and most ANNs on ModelNet40 and ScanObjectNN. Besides point-based networks, E-3DSNN (Qiu et al., 2025) explored

sparse spike convolution on voxels, imitating the aforementioned MS-ResNet (Hu et al., 2024). E-3DSNN achieved unprecedented results on ModelNet40, surpassing all three point-based SNN baselines for the first time.

2.3. Unified Methods for 3D cloud Analysis

Most importantly, both (Lan et al., 2023) and E-3DSNN follow the philosophy of unified design for multi-task learning. They rethink network design not only for point clouds but also for other data types. The conversion method was universal, enabling the acquisition of SNN versions of PointNet, PointNet++, VGG-16 and ResNet-20. E-3DSNN effectively applied 2D convolution to both 3D voxels and 2D pixels of event streams. We also adhere to the philology of unified design for both event clouds and point clouds.

3. Method

3.1. Event-driven PointNet

As shown in Figure 2, The top illustrates Spiking PointNet proposed by (Ren et al., 2023a), which follows a conventional timestep-wise iterative activation mechanism. This approach requires an additional temporal dimension T on top of the batch size B , channel size C , and total number of points N . As a direct consequence, most vision data processed in SNNs consume T times more memory compared to ANN-based models. Moreover, since activations are updated step by step, both training and inference in SNNs are inherently slower than in ANNs. The bottom illustrates our proposed AMP2-based event-driven PointNet model. AMP2 enables SNNs to function like ANNs while maintaining event-driven characteristics. It ensures data sparsity, preventing the memory overhead from scaling by a factor of T , thereby significantly improving efficiency.

3.2. Spiking Activation Function

The leaky integrate-and-fire (LIF) model is one of the most commonly used spiking activation functions, as it balances historical information and current features. Its mathematical form is typically described by Equation (2), Equation (3) and Equation (4).

$$U_l^t = H_l^{t-1} + X_l^t \quad (2)$$

$$S_l^t = \text{Hea.}(U_l^t - V_{th}) \quad (3)$$

$$H_l^t = \beta U_l^t \odot (1 - S_l^t) + u_{th} S_l^t \quad (4)$$

where l and t denote the layer and timestep, U_l^t means the accumulated membrane potential at t , namely, the membrane potential (MP) prior to spiking activation. The accumulated value consists of two items, the MP after spiking activation at $t - 1$, H_l^{t-1} , and the t th processed feature, X_l^t , from the l th layer’s input, processing could be convolution operation,

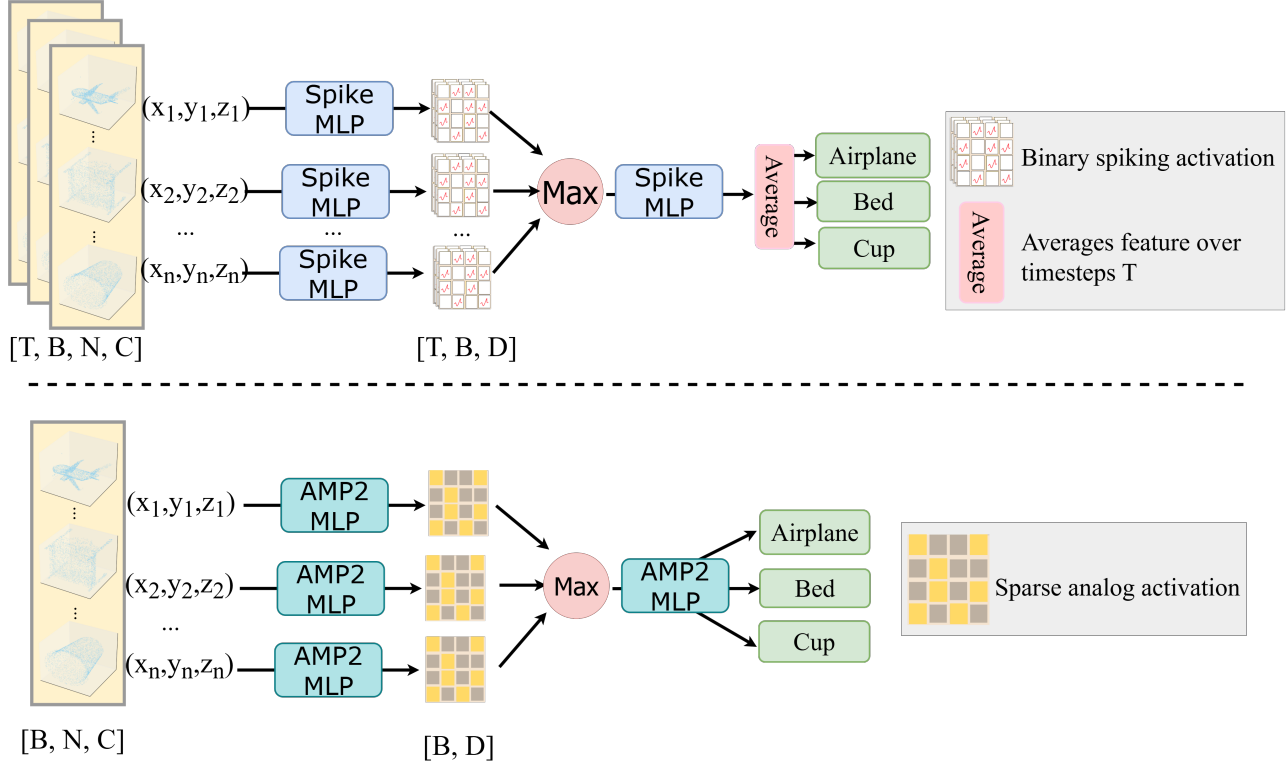


Figure 2. Overview of event-driven PointNet for 3D object classification. The top demonstrates the workflow of Spiking PointNet, using binary value 0, 1 to discriminate features; the bottom part illustrates event-based computation without timestep-wise activation, which exploits sparse analog value for forward propagation, the yellow cell in the grid represents inactive state 0, the gray cell indicates non-linear activation.

MLP and so forth. u_{th} is the rest potential which is set after activating the output spikes, we call it hard reset when $u_{th} = 0$. V_{th} represents the threshold to determine whether the output spikes S_l^t should be fired or stay inactive. $Hea(\cdot)$ is a Heaviside step function that satisfies $Hea(x) = 1$ when $x \geq 0$, otherwise $Hea(x) = 0$. Besides, the leaky function depends on the decay factor $\beta = e^{-\frac{dt}{\tau}} \in (0, 1)$ to decrease the impact of historical information, while τ reflects the membrane time constant. \odot denotes the element-wise multiplication.

In practice, the spiking activation function could output pure binary spikes (0, 1) or sparse non-binary values. The latter can be implemented in various ways, such as using firing rate encoding, where the accumulated spikes are summed and averaged over timesteps. Another method is $S_l \odot V_{th}$, where the spike values are multiplied by the corresponding V_{th} . This approach often achieves better performance with dynamic thresholds. Our proposed AMP2 method multiplies the spike values by the membrane potential prior to activation U_l . This approach is the first step towards eliminating timestep-wise iterative computation. A complete spiking

Algorithm 1 AMP2-LIF Activation

Input: feature X , previous layer’s post-spike membrane potential H_{l-1} , threshold V_{th} , coefficients α and β

if H_{l-1} is None **then**

$H_l^0 \leftarrow$ randomly initialized value

else

$H_l^0 \leftarrow \alpha \cdot H_{l-1} + (1 - \alpha) \cdot$ random value

end if

$U_l \leftarrow H_l^0 + X$

$S_l \leftarrow Heaviside(U_l - V_{th})$

$H_l \leftarrow \beta \cdot U_l \odot (1 - S_l) + u_{th} \cdot S_l$

Output: $S_l \odot U_l, H_l$

module of AMP2 can be summarized by Equation (5).

$$LIF_{AMP2}(\Phi(x_l)) = S_l(w_l \cdot x_l + b_l) \odot U_l(w_l \cdot x_l + b_l) \quad (5)$$

where w_l and b_l represent the weight and bias of processing operation within this module.

3.3. Activation-wise Membrane Potential Propagation

Figure 6 illustrates the detailed propagation process of

AMP2 within the network. AMP2 redefines the timestep not as an independent iterative computation within each spiking activation function, but as a shared parameter among activation functions at different depths within the network. This approach has several advantages: firstly, it allows the membrane potentials of activation functions operating at different ranges to be interconnected, stabilizing the gradient during SNN training; secondly, the sparse non-binary output values of AMP2-LIF still adhere to the event-driven computation nature, and using the pre-spike membrane potential U_l helps reduce the loss of effective feature values caused by spiking. Algorithm 1 demonstrates the membrane potential update and spike generation mechanism based on the AMP2 algorithm, α is set to 0.8 in all experiments.

We recognize that AMP2 may appear similar to the residual connections studied in previous works on spiking networks. The key difference is that AMP2 connects the membrane potential parameter within the LIF activation function, whereas residual connections link feature values across different layers. The performance differences between these two approaches can be observed in the ablation study in Section 4.4.2.

4. Experiment

Only a few related researches have their code open-sourced on the Internet. We chose the Spiking PointNet proposed by (Ren et al., 2023a) as our SNN baseline for most experiments. The details of the point cloud experiments and ANN model follow (Yan, 2019). As for event cloud data, we investigate AMP2 on event frames and event points. For frame data, we referred to the code from (Fang et al., 2021), and for processing the raw DVS data into event clouds, we referred to the code from (Wang et al., 2019).

4.1. Power Consumption on Neuromorphic Processor

To investigate the practical impact of timesteps on spiking networks, we conducted detailed power consumption experiments on the neuromorphic chip Lynxi HP201. Figure 3 records the inference time for different models processing one batch from the ModelNet40 dataset on HP201 chip. It can be observed that larger timesteps significantly increase the computation latency for 3D object recognition in spiking networks. Unsurprisingly, the ANN-based PointNet achieved the shortest inference time, while the MP PointNet took longer than the Spiking PointNet ($T=1$). We speculate that this is because the tested MP PointNet was an early development version with many redundant computations and insufficient algorithm optimization. Theoretically, the MP PointNet using AMP2 should have a similar inference time to the $T=1$ model. Table 1 details the power consumption (mW) of the processor during inference. It is important to note that to run both ANN and SNN models uniformly,

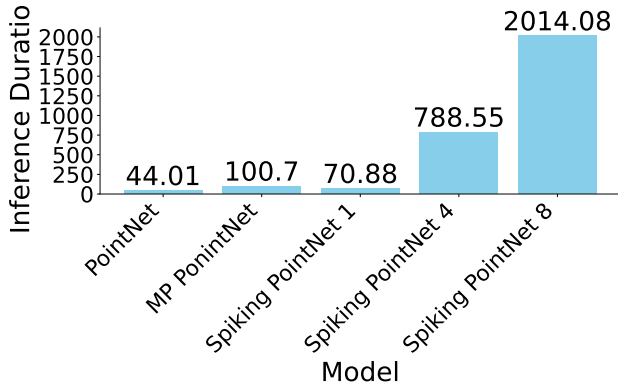


Figure 3. Inference durations (seconds) for various models on a batch from the ModelNet40 test set, conducted on a lynxi HP201 computing unit. The recorded times represent only the Inference phase as detailed in Table 1. Each bar displays the specific inference duration at the top. Note that the MP PointNet results are overestimated, as the tested MP PointNet is an early, unoptimized version with some unnecessary computations.

all code was compiled and executed using the HP201’s PyTorch-compatible interface, and the SNN network did not utilize the HP201’s specialized neuromorphic computation instruction interface. Therefore, the power consumption does not reflect the true power usage of SNN on neuromorphic processor. We found that with a standby power consumption of approximately 14.5W for the entire chip, the ANN network, while having a lower base power consumption during inference, exhibited significant peak power fluctuations. In contrast, the SNN had a slight higher base power consumption due to iterative activations but showed more stable power variations. The MP PointNet achieved both lower base power consumption and stable peak power consumption.

4.2. Point Cloud Analysis

4.2.1. CLASSIFICATION

We tested the original Spiking PointNet on more datasets and expanded it onto single scale grouping (SSG) version of PointNet++ in Table 2. Spiking PointNet seems to be overfitting on the OBJ_BG variant of ScanObjectNN main split when $T = 1$. Although AMP2 did not enable the SNN to directly outperform the original PointNet with the same structure, it brought significant performance improvements regardless of whether the backbone was PointNet or PointNet++. Moreover, AMP2 outperformed the recent voxel-based SNN state-of-the-art model, E-3DSNN with MP PointNet2.

Table 1. Average power consumption (mW) and standard deviation before (Pre), during, and after (Post) inference on a batch from the ModelNet40 test set using the Lynix HP201. The sampling duration for before and after inference is 10 seconds each. The during inference sampling starts after loading the model and data, and ends when inference is complete. Note that the power consumption of MP PointNet is overestimated due to some unnecessary computations in the tested version.

Type	Model	timestep	Pre	Inference	Post
SNN	Spiking PointNet	1	15262.50 ± 33.08	15669.20 ± 209.0	15294.0 ± 0.0
		4	15311.75 ± 22.82	15912.54 ± 60.88	15459.50 ± 251.47
		8	15217.25 ± 8.67	15954.18 ± 49.49	15339.50 ± 4.33
	MP PointNet	-	15263.75 ± 22.82	15770.90 ± 184.70	15281.25 ± 4.76
ANN	PointNet	-	14698.50 ± 6.38	15267.47 ± 290.63	14708.25 ± 12.66

Table 2. Object recognition on classification benchmarks. * indicates that the results for the model are extracted from the corresponding original paper.

Backbone	Model	Type	T	ModelNet40		ScanObjectNN(OBJ_BG)		ScanObjectNN(PB_T50_RS)	
				OA	mACC	OA	mACC	OA	mACC
PointNet	(Yan, 2019)	ANN	-	90.43	86.66	68.40	62.38	55.87	50.24
			1	86.59	81.34	24.84	26.51	52.32	47.59
	Spiking PointNet	SNN	4	88.41	83.43	-	-	-	-
			8	88.50	84.73	-	-	-	-
	MP PointNet	SNN	-	89.56	84.91	64.46	60.51	55.19	50.79
(Lan et al., 2023)*	SNN	16	88.17	-	66.56	-	-	-	
PointNet++	SSG (Yan, 2019)	ANN	-	92.33	90.07	84.46	82.62	78.83	77.24
			1	87.36	82.58	48.01	43.77	66.74	63.73
	Spiking PointNet2	SNN	4	91.22	87.43	-	-	-	-
			8	91.61	88.59	-	-	-	-
	MP PointNet2	SNN	-	92.36	90.09	85.58	82.13	78.24	76.19
(Lan et al., 2023)*	SNN	16	89.45	-	69.22	-	-	-	
-	P2SResLNet*	SNN	1	90.60	89.20	81.20	79.40	-	-
-	E-3DSNN*	SNN	1	91.70	-	-	-	-	-

Table 3. Performance comparison on the ShapeNetPart dataset for part segmentation. The evaluation metrics is mean Intersection over Union (mIoU, %), including the best instance mIoU, best category mIoU, and per-category mIoU achieved by model with the best instance mIoU. We compare PointNet, Spiking PointNet, and MP PointNet with our proposed AMP2. Full results can be found in Appendix A

mIoU	PointNet	Spiking PointNet	MP PointNet
Instance	84.48	78.46	82.66
Category	80.61	72.76	78.53

4.2.2. PART SEGMENTATION

In Table 3, we also found that AMP2 directly brought about a 6% improvement in object segmentation for Spiking PointNet on the ShapeNet-Part dataset, although there is still a 2% gap compared to PointNet.

4.2.3. SEMANTIC SEGMENTATION

On the 3D indoor parsing dataset (S3DIS), the performance gap between MP PointNet and PointNet further narrowed

to less than 2%, with MP PointNet outperforming Spiking PointNet by a margin of 6% to 8%.

Table 4. Best accuracy (%) and mIoU (%) on the 3D Indoor Parsing Dataset (S3DIS). The per-category IoU values were achieved by model with the highest category mIoU. Full results can be found in Appendix B

	Metric	PointNet	Spiking PointNet	MP PointNet
Acc.	instance	79.59	70.66	78.48
	class	54.38	46.10	53.04
IoU	Mean	43.20	34.53	41.98

4.3. Event Cloud Analysis

4.3.1. EVENT FRAME RECOGNITION

In models analyzing event frame data, the raw event stream needs to be integrated into frames with a number consistent with the timesteps. This pixelization of DVS data is a commonly used processing method within the community.

Table 5. Improvement of AMP2 on framed DVS128 Gesture dataset

Backbone	AMP2	Top1 Acc.(%)	Top5 Acc.(%)
SEWResNet	✓	90.63	99.65
	×	88.19	100.0
PlainNet	✓	80.56	99.31
	×	75.0	99.65
SpikingResNet	✓	17.01	49.65
	×	71.88	99.31

The length of the timesteps directly affects the quality of the frame data integrated from the raw event stream; naturally, longer timesteps will convert into richer pseudo-pixel data. Due to this, the input data will vary significantly under different timesteps. We uniformly use $T=4$ and employ the small versions of three models from (Fang et al., 2021): SEWResNet, PlainNet, and SpikingResNet, as the subjects of our experiments. We compare the impact of AMP2 on the data sampled from the DVS128Gesture frames, with the results shown in Table 5. It can be observed that, apart from SpikingResNet, the other two models benefit from the performance improvements brought by the introduction of AMP2.

4.3.2. EVENT POINT RECOGNITION

Using the sliding window method from (Wang et al., 2019), we set the window size to 0.5 and the step size to half of the window size, 0.25. To avoid the coupling of timesteps and input, we segmented the raw event streams into a complete set of event clouds, downsampling 1024 event points from each event stream and discarding the random class from the DVS128 Gesture dataset. We tested the PointNet model’s performance in recognizing event clouds across 10 distinct categories. As shown in Table 6, AMP2 achieves competitive performance with ANN under the same model structure. Although it lags behind the $T=4$ Spiking PointNet, it surpasses it in the PointNet++ architecture.

Table 6. Classification accuracies for 10-class DVS128 Gesture.

Backbone	Type	Model	T	OA	mACC
PointNet	ANN	(Yan, 2019)	-	89.57	89.21
		(Wang et al., 2019)	-	89.68	-
	SNN	Spiking PointNet	1	31.22	32.58
			4	91.32	90.15
		MP PointNet	-	89.64	89.49
PointNet++	ANN	(Yan, 2019)	-	96.74	95.85
		(Wang et al., 2019)	-	95.89	-
	SNN	Spiking PointNet2	1	85.00	84.57
			4	94.68	94.25
		MP PointNet2	-	96.35	96.33

4.4. Ablation

4.4.1. SPIKING POINTNET $T = 1, 4, 8$

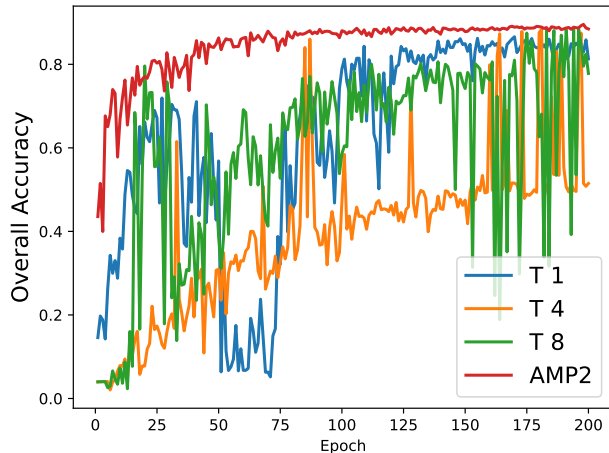


Figure 4. Classification accuracy of PointNet-based models on the ModelNet40 without voting. The models compared are Spiking PointNet (SNN baseline, $T = 1, 4, 8$ and MP PointNet (using AMP2)

Out of curiosity, for the proposed Spiking PointNet, we compared the traditional timestep-wise activation with the AMP2 method on PointNet (Figure 4) and PointNet++ (Figure 5). The training gradients of SNN in the PointNet architecture are extremely unstable, and even with $T=8$, there is no significant improvement compared to $T=1$. However, PointNet++ clearly demonstrates the benefits of longer timesteps, although neither can surpass AMP2.

4.4.2. RESIDUAL CONNECTION

Table 7. Classification accuracy (%) of residual connection and AMP2 on PointNet architecture, evaluated on ModelNet40.

Model	T	OA	mACC
MP PointNet	-	89.56	84.91
SpikeRC PointNet	1	65.90	61.70
	4	88.78	84.46

We replaced AMP2 with residual connections in PointNet, resulting in SpikeRC PointNet. We tested it with $T=1$ and $T=4$, and the results after training for 200 epochs on the ModelNet40 dataset are reported in Table 7. AMP2 slightly outperforms the $T=4$ SpikeRC PointNet.

5. Conclusions

In this work, we propose a novel, simple yet highly effective update strategy for spiking activation functions in spiking

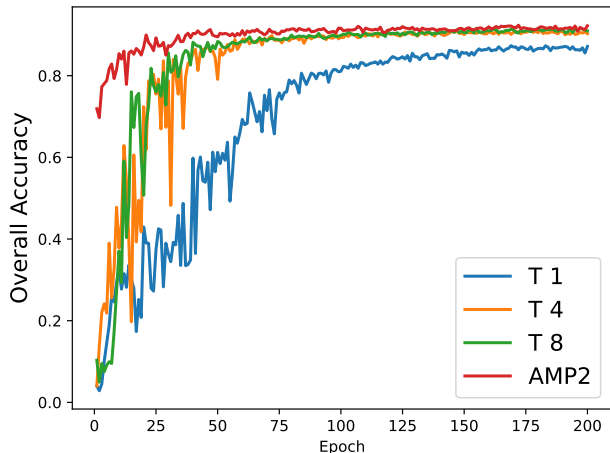


Figure 5. Classification accuracy of PointNet++(ssg) based models on the ModelNet40 without voting. The models compared are Spiking PointNet2 (SNN baseline, $T = 1, 4, 8$ and MP PointNet2 (using AMP2)

neural networks, termed activation-wise membrane potential propagation (AMP2). Unlike the traditional approach of iteratively updating membrane potentials and generating spike values at each timestep, AMP2 outputs the accumulated membrane potential prior to spike generation and directly transmits the post-spike membrane potential to the next layer’s activation function. This method transforms the sparse analog values from temporal computation to spatial computation, allowing activation functions within the same module to share a unified timestep parameter. This parameter is no longer manually designed but is instead bound to the network’s depth.

Through extensive experiments, we demonstrate that this strategy significantly improves performance in both point cloud analysis and DVS event cloud recognition. For instance, AMP2 achieves competitive performance with ANN models and outperforms recent voxel-based SNN models like E-3DSNN. Additionally, AMP2 shows substantial improvements in object segmentation on the ShapeNet-Part dataset and narrows the performance gap with PointNet on the S3DIS dataset. However, we also observe that AMP2 does not universally enhance performance across all model structures. For example, in Spiking ResNet, AMP2 leads to a performance decline. This raises intriguing questions about the applicability of AMP2 in traditional visual data and other model architectures. Future work will explore the broader applicability of AMP2 across various model structures and datasets to further validate its effectiveness and identify potential limitations.

References

- Amir, A., Taba, B., Berg, D., Melano, T., McKinstry, J., Di Nolfo, C., Nayak, T., Andreopoulos, A., Garreau, G., Mendoza, M., et al. A low power, fully event-based gesture recognition system. In *Proceedings of the IEEE conference on computer vision and pattern recognition*, pp. 7243–7252, 2017.
- Bi, Y., Chadha, A., Abbas, A., Bourtsoulatze, E., and Andreopoulos, Y. Graph-based spatio-temporal feature learning for neuromorphic vision sensing. *IEEE Transactions on Image Processing*, 29:9084–9098, 2020.
- Cheng, Y., Su, J., Jiang, M., and Liu, Y. A novel radar point cloud generation method for robot environment perception. *IEEE Transactions on Robotics*, 38(6):3754–3773, 2022.
- Cui, Y., Chen, R., Chu, W., Chen, L., Tian, D., Li, Y., and Cao, D. Deep learning for image and point cloud fusion in autonomous driving: A review. *IEEE Transactions on Intelligent Transportation Systems*, 23(2):722–739, 2022. doi: 10.1109/TITS.2020.3023541.
- Duan, H., Wang, P., Huang, Y., Xu, G., Wei, W., and Shen, X. Robotics dexterous grasping: The methods based on point cloud and deep learning. *Frontiers in Neurorobotics*, 15:658280, 2021.
- Fang, W., Yu, Z., Chen, Y., Huang, T., Masquelier, T., and Tian, Y. Deep residual learning in spiking neural networks. *Advances in Neural Information Processing Systems*, 34:21056–21069, 2021.
- Hu, Y., Deng, L., Wu, Y., Yao, M., and Li, G. Advancing spiking neural networks toward deep residual learning. *IEEE Transactions on Neural Networks and Learning Systems*, pp. 1–15, 2024. doi: 10.1109/TNNLS.2024.3355393.
- Lan, Y., Zhang, Y., Ma, X., Qu, Y., and Fu, Y. Efficient converted spiking neural network for 3d and 2d classification. In *Proceedings of the IEEE/CVF International Conference on Computer Vision*, pp. 9211–9220, 2023.
- Lee, J. H., Delbruck, T., Pfeiffer, M., Park, P. K., Shin, C.-W., Ryu, H., and Kang, B. C. Real-time gesture interface based on event-driven processing from stereo silicon retinas. *IEEE transactions on neural networks and learning systems*, 25(12):2250–2263, 2014.
- Ma, X., Qin, C., You, H., Ran, H., and Fu, Y. Rethinking network design and local geometry in point cloud: A simple residual mlp framework. In *The International Conference on Learning Representations*, 2022.
- Mei, L., Wang, S., Cheng, Y., Liu, R., Yin, Z., Jiang, W., Wang, S., and Gong, W. Esp-pct: Enhanced vr semantic performance through efficient compression of temporal and spatial redundancies in point cloud transformers. In Larson, K. (ed.), *Proceedings of the Thirty-Third International Joint Conference on Artificial Intelligence, IJCAI-24*, pp. 1182–1190. International Joint Conferences on Artificial Intelligence Organization, 8 2024. doi: 10.24963/ijcai.2024/131. URL <https://doi.org/10.24963/ijcai.2024/131>. Main Track.
- Qi, C. R., Su, H., Mo, K., and Guibas, L. J. Pointnet: Deep learning on point sets for 3d classification and segmentation. In *Proceedings of the IEEE Conference on Computer Vision and Pattern Recognition (CVPR)*, July 2017a.
- Qi, C. R., Yi, L., Su, H., and Guibas, L. J. Pointnet++: Deep hierarchical feature learning on point sets in a metric space. *Advances in neural information processing systems*, 30, 2017b.
- Qiu, X., Yao, M., Zhang, J., Chou, Y., Qiao, N., Zhou, S., Xu, B., and Li, G. Efficient 3d recognition with event-driven spike sparse convolution. In *Proceedings of the Thirty-Ninth AAAI Conference on Artificial Intelligence*, 2025.
- Qiu, Z., Yao, T., and Mei, T. Learning spatio-temporal representation with pseudo-3d residual networks. In *proceedings of the IEEE International Conference on Computer Vision*, pp. 5533–5541, 2017.
- Ren, D., Ma, Z., Chen, Y., Peng, W., Liu, X., Zhang, Y., and Guo, Y. Spiking pointnet: spiking neural networks for point clouds. In *Proceedings of the 37th International Conference on Neural Information Processing Systems, NIPS '23*, Red Hook, NY, USA, 2023a. Curran Associates Inc.
- Ren, H., Zhou, Y., Fu, H., Huang, Y., Xu, R., and Cheng, B. Tpoint: A tensorized point cloud network for lightweight action recognition with event cameras. In *Proceedings of the 31st ACM International Conference on Multimedia*, pp. 8026–8034, 2023b.
- Ren, H., Zhou, Y., Huang, Y., Fu, H., Lin, X., Song, J., and Cheng, B. Spikepoint: An efficient point-based spiking neural network for event cameras action recognition. *arXiv preprint arXiv:2310.07189*, 2023c.
- Sekikawa, Y., Hara, K., and Saito, H. Eventnet: Asynchronous recursive event processing. In *Proceedings of the IEEE/CVF conference on computer vision and pattern recognition*, pp. 3887–3896, 2019.

- Shen, G., Zhao, D., and Zeng, Y. Eventmix: An efficient data augmentation strategy for event-based learning. *Information Sciences*, 644:119170, 2023.
- Thomas, H., Qi, C. R., Deschaud, J.-E., Marcotegui, B., Goulette, F., and Guibas, L. J. Kpconv: Flexible and deformable convolution for point clouds. In *Proceedings of the IEEE/CVF international conference on computer vision*, pp. 6411–6420, 2019.
- Wang, Q., Zhang, Y., Yuan, J., and Lu, Y. Space-time event clouds for gesture recognition: From rgb cameras to event cameras. In *2019 IEEE Winter Conference on Applications of Computer Vision (WACV)*, pp. 1826–1835. IEEE, 2019. URL https://github.com/qwang014/EVclouds_gesture_recognition.
- Wang, Q., Zhang, Y., Yuan, J., and Lu, Y. St-evnet: Hierarchical spatial and temporal feature learning on space-time event clouds. *Proc. Adv. Neural Inf. Process. Syst. (NeurIPS)*, 2020.
- Wu, Q., Zhang, Q., Tan, C., Zhou, Y., and Sun, C. Point-to-spike residual learning for energy-efficient 3d point cloud classification. In *Proceedings of the AAAI Conference on Artificial Intelligence*, volume 38, pp. 6092–6099, 2024.
- Wu, Z., Song, S., Khosla, A., Yu, F., Zhang, L., Tang, X., and Xiao, J. 3d shapenets: A deep representation for volumetric shapes. In *Proceedings of the IEEE conference on computer vision and pattern recognition*, pp. 1912–1920, 2015.
- Yan, X. Pointnet/pointnet++ pytorch. https://github.com/yanx27/Pointnet_Pointnet2_pytorch, 2019.
- Yao, M., Hu, J., Zhou, Z., Yuan, L., Tian, Y., XU, B., and Li, G. Spike-driven transformer. In *Thirty-seventh Conference on Neural Information Processing Systems*, 2023a. URL <https://openreview.net/forum?id=9FmolyOHi5>.
- Yao, M., Zhang, H., Zhao, G., Zhang, X., Wang, D., Cao, G., and Li, G. Sparser spiking activity can be better: Feature refine-and-mask spiking neural network for event-based visual recognition. *Neural Networks*, 166:410–423, 2023b.
- Yao, M., Hu, J., Hu, T., Xu, Y., Zhou, Z., Tian, Y., XU, B., and Li, G. Spike-driven transformer v2: Meta spiking neural network architecture inspiring the design of next-generation neuromorphic chips. In *The Twelfth International Conference on Learning Representations*, 2024a. URL <https://openreview.net/forum?id=1SIBN5Xyw7>.
- Yao, M., Qiu, X., Hu, T., Hu, J., Chou, Y., Tian, K., Liao, J., Leng, L., Xu, B., and Li, G. Scaling spike-driven transformer with efficient spike firing approximation training. *arXiv preprint arXiv:2411.16061*, 2024b.
- Zhou, Z., Zhu, Y., He, C., Wang, Y., YAN, S., Tian, Y., and Yuan, L. Spikformer: When spiking neural network meets transformer. In *The Eleventh International Conference on Learning Representations*, 2023. URL https://openreview.net/forum?id=frE4fUwz_h.
- Zhou, Z., Che, K., Fang, W., Tian, K., Zhu, Y., Yan, S., Tian, Y., and Yuan, L. Spikformer v2: Join the high accuracy club on imagenet with an snn ticket. *arXiv preprint arXiv:2401.02020*, 2024.
- Zieliński, K., Blumberg, B., and Kjærgaard, M. B. Precise workcell sketching from point clouds using an ar toolbox. In *2024 33rd IEEE International Conference on Robot and Human Interactive Communication (ROMAN)*, pp. 1754–1760. IEEE, 2024.

A. Supplementary results on ShapeNet-Part

Table 8. Performance comparison on the ShapeNetPart dataset for part segmentation. The evaluation metrics is mean Intersection over Union (mIoU, %), including the best instance mIoU, best category mIoU, and per-category mIoU achieved by model with the best instance mIoU. We compare PointNet, Spiking PointNet, and MP PointNet with our proposed AMP2.

mIoU	PointNet	Spiking PointNet	MP PointNet
Instance	84.48	78.46	82.66
Category	80.61	72.76	78.53
Airplane	82.89	73.94	79.86
Bag	77.44	64.75	73.71
Cap	81.52	72.50	77.06
Car	77.18	63.89	73.10
Chair	90.17	85.81	88.67
Earphone	71.07	67.89	71.36
Guitar	90.93	83.23	89.42
Knife	86.39	80.69	83.31
Lamp	80.68	73.58	78.13
Laptop	95.49	93.91	94.63
Motorbike	65.60	50.87	63.36
Mug	93.19	83.33	91.27
Pistol	82.41	74.90	78.93
Rocket	54.21	47.98	54.48
Skateboard	74.32	63.72	71.91
Table	82.60	78.99	81.78

B. Supplementary results on S3DIS

Table 9. Best accuracy (%) and mIoU (%) on the 3D Indoor Parsing Dataset (S3DIS). The per-category IoU values were achieved by model with the highest category mIoU.

	Metric	PointNet	Spiking PointNet	MP PointNet
Acc.	instance	79.59	70.66	78.48
	class	54.38	46.10	53.04
IoU	Mean	43.20	34.53	41.98
	ceiling	88.5	81.3	87.6
	floor	97.6	88.3	96.5
	wall	70.2	58.7	70.3
	beam	0.1	0	0.1
	column	8.1	2.8	0.6
	window	50.9	34.1	47.6
	door	8	12.6	11.3
	table	54.6	40.1	55.5
	chair	43.8	40.6	45.6
	sofa	16.3	7.9	8.5
	bookcase	54.3	38.3	51.9
	board	37.2	19.7	38.0
	clutter	32.1	24.5	32.3

C. Illustration of AMP2

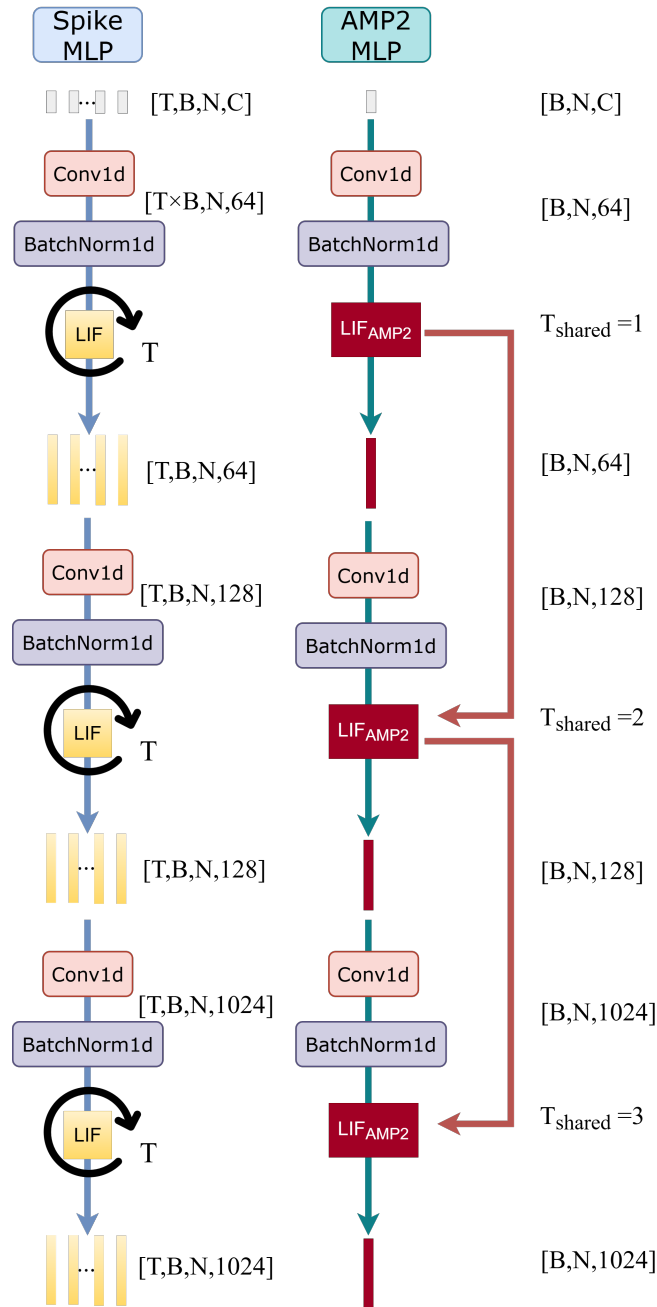


Figure 6. Comparison of timestep-wise iterative activation and Activation-wise Membrane Potential Propagation in a 3-layer MLP. The left side illustrates the commonly used MP update method, which requires T computations within the LIF for MP updates. The right side shows our proposed AMP2 update strategy, where the post-spike membrane potential H_i of the LIF within the module is propagated forward between activation layers. Unlike the traditional method where each activation function has its own separate timestep computations, we extend the timestep across the network depth, allowing activation functions at different positions within the same module to share a single timestep parameter.